Volume-size distribution of microparticles in ice cores from the Tibetan Plateau

Guangjian WU,[1] Tandong YAO,[1,2] Baiqing XU,[1] Lide TIAN,[1,2] Chenglong ZHANG,[1] Xuelei ZHANG[1]

[1]*Key Laboratory of Tibetan Environment Changes and Land Surface Processes, Institute of Tibetan Plateau Research, Chinese Academy of Sciences, 18 Shuangqing Road, Beijing 100085, China*
E-mail: wugj@itpcas.ac.cn
[2]*State Key Laboratory of Cryospheric Science, Chinese Academy of Sciences, Lanzhou 730000, China*

ABSTRACT. The volume distribution of atmospheric dust particles (microparticles) of 1–30 μm diameter in Muztagata, Dunde, Dasuopu and Everest ice cores from the Tibetan Plateau was measured and fitted as a log-normal function in order to characterize their basic size properties. Our results reveal that whether the volume distribution fits the log-normal function or not largely depends on the dust concentration and the specific dust-storm event but is independent of physiographical location and season. Our results show only high-concentration samples obey the log-normal distribution in volume, with mode sizes ranging from 3 to 16 μm. The log-normal distribution was largely attributed to the mid-sized particles between 3 and 15 μm, which contribute most (>70%) of the total volume. The volume size distribution characteristics for mineral dust particles from ice cores reveal that the coarse particles might be common in the upper-level troposphere over the Tibetan Plateau. These dust size features are useful to advance our understanding of dust effects on climate, and provide clues to better characterize atmospheric dynamics over the Tibetan Plateau that will help to improve the current models.

INTRODUCTION

The properties of atmospheric dust are key parameters in the assessment of their climatic impact. Studies of the cycling of mineral particles through the environment have shown that the size distributions of atmospheric dust particles are sensitive to climate processes (Arimoto and others, 1997). Eolian dust grain size is a proxy for the wind strength that entrains it. Grain sizes and their distribution characteristics in ice cores have been used to reflect the wind strength and dust storms in source areas (Steffensen, 1997; Zielinski and others, 1997; Ruth and others, 2003); used as a proxy for winter monsoon strength in Chinese loess deposits (Porter and An, 1995; Zhang and others, 1999); and taken as a signal of the wind strength and transport dynamics in deep-sea eolian sediments (Rea and Hovan, 1995).

The central Asian region is one of the major global dust-source areas in the Northern Hemisphere. Recently, dust aerosol over the Tibetan Plateau has been hypothesized, based on modeling results (Lau and others, 2006), to be an important factor in the Asian summer monsoon, largely by affecting the radiation balance by absorbing and scattering solar radiation (Huang and others, 2007). Being adjacent to the central Asian arid regions, glaciers on the Tibetan Plateau provide a unique medium for preserving atmospheric dust deposits, and contribute an excellent record of environmental change and atmospheric processes. Particle grain-size distribution also reflects the transport mechanisms. Size distribution characteristics of atmospheric dust on the Tibetan Plateau might differ from those in remote deposition sites (e.g. Greenland). Junge (1977) has assumed a near-uniform background aerosol at altitudes more than ~5 km a.s.l. over the continents. The surface of the Tibetan Plateau is higher than 4 km a.s.l. Ice-core drilling sites are close to or more than 6 km a.s.l., where the size distribution of atmospheric dust might be more complex than Junge's assumption. The Tibetan Plateau itself is thought by some researchers (e.g. Fang and others, 2004) to be an important source region for Asian dust. Thus, the dust over the Tibetan Plateau may differ from that in remote deposition sites. Compared with studies in polar regions, size distribution measurements in ice and snow on the Tibetan Plateau are scarce (Wake and others, 1994; Wu and others, 2006) and are insufficient to enunciate the properties of atmospheric dust in detail, owing to either the limitations of short time series or site availability. In addition, it is likely that the size distribution of dust particles in ice cores is more complex than being simply controlled by geographical location. Due to the vast region and variable environment across the Tibetan Plateau, dusts deposited in ice and snow at different sites might show different characteristics in their grain size and distribution, as well as in their concentration.

Lack of knowledge about the size distribution of dust is an obstacle to understanding the dust's radiative properties and transport dynamics (e.g. Tegen and Lacis, 1996). The assumed dust size in many general climate models seems too simplified and notably deviates from actual data. One main impetus for the present work is to provide a better understanding of the basic properties of the size distribution of eolian dust particles in the atmosphere, which will facilitate more quantitative interpretations of the dust record in ice cores on the Tibetan Plateau and the climatic impacts of dust particles in general climate models. This study discusses the volume size distribution of microparticles in several ice cores recovered at different geographical sites on the Tibetan Plateau, and compares the size distribution parameters with those from Greenland as the end member of the Asian dust. All grain sizes in this paper are particle diameters unless specified otherwise.

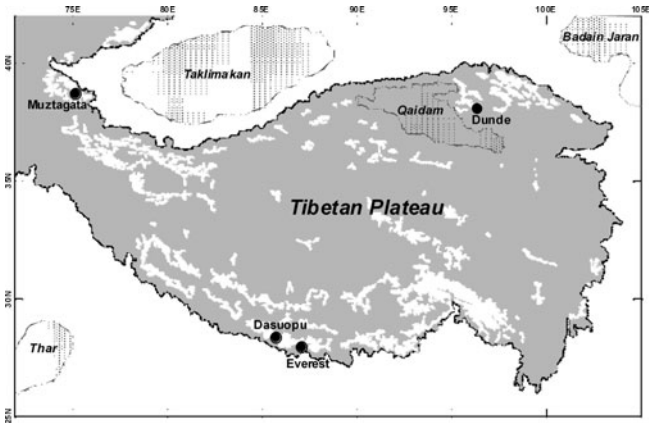

Fig. 1. Location map for the ice-core sites for microparticle analysis on the Tibetan Plateau.

GEOGRAPHICAL SETTING, SAMPLING AND EXPERIMENTAL PROCEDURES

The Tibetan Plateau is enclosed by arid regions to the north (e.g. the Taklimakan, Gobi and Badain Jaran deserts), the west (e.g. Iran–Afghanistan, west Asia) and the south (the Thar desert and Indian subcontinent). Westerlies dominate the climate regime in the Pamirs, whereas both the Indian monsoon and the westerlies affect the Himalayan region (Fig. 1). Source areas for dust in Tibetan Plateau ice cores have been described by Wake and others (1994). In the northern part of the Tibetan Plateau, dust comes mostly from northern China and the Gobi desert (Thompson and others, 1988). In the Pamirs, the dust most likely comes from around the glacierized area and the west Asian arid regions (Wake and others, 1994; Wu and others, 2009). In the southern part of the Tibetan Plateau, dust sources are mainly located in the Indian subcontinent and further from central Asia (Shrestha and others, 2000; Carrico and others, 2003).

We have drilled several ice cores on the Tibetan Plateau during the past decade. During the 2001–03 summer seasons, several ice cores from the glacial accumulation zone at 6250, 6350 and 7010 m a.s.l. (Tian and others, 2006) were recovered on Muztagata (38°17′ N, 75°04′ E), eastern Pamirs. This study discusses microparticle records from three ice-core sections, as follows: the upper 7.89 m (dating from 2001 to 1998) of a 93.5 m core drilled at 6250 m a.s.l.; 44.31 m of core (about 40 years) from 6350 m a.s.l.; and the upper 33.68 m (about 33 years) of a 54.5 m core from 7010 m a.s.l.

The Dunde ice cap, located in a desert environment between the Qaidam basin (the highest desert in China) and the Gobi desert, is strongly impacted by the east Asian winter monsoon. In October 2002, five shallow ice cores were recovered near a site that was drilled to the bedrock in 1987 (Thompson and others, 1988). The dust from one of the shallow cores, 17.37 m long and covering about 30 years, was analyzed for concentrations and size distributions.

In May 2005, three ice cores were drilled in East Rongbuk Glacier (27°59′ N, 86°55′ E; 6450 m a.s.l.) on the northern slope of Mount Everest (Qomolangma). An ice core, with length 22.45 m (about 40 years), was analyzed for oxygen isotopes, microparticles and ions. In August 2006, a short firn core with depth 17.21 m (dated 1991–2005) was recovered from Dasuopu glacier (28°23′ N, 85°44′ E; 7000 m a.s.l.), Xixiabangma mountain.

The cores were kept frozen and sampled at intervals of 4–6 cm. Oxygen isotope ratios (using Vienna Standard Mean Ocean Water (V-SMOW) as reference) were measured by MAT-252 and Delta-Plus mass spectrometers, with a precision better than ±0.5‰. The microparticles were measured in a class 1000 clean room under a class 100 clean hood using a Beckman Multisizer 3 Coulter Counter with a 50 μm diameter aperture, counting in 256 or 300 channels between 1 and 30 μm on a logarithmic scale. Most of the samples were measured within 4 hours of melting, with the exception of a very few samples which were measured after 1 or 2 days due to power failure. Particle sizes given here are spherical equivalent diameters. In our experience, particle number concentrations in the range 10^4–10^5 mL^{-1} seemed most suitable for measurement. Because of the high particle concentrations, all samples were diluted two to five times using ISOTON II electrolyte before measurement. For a few extremely high-concentration samples, the dilution ratios reached 25 times. The measurement was calibrated using standard nominal polystyrene latex particles. The background levels of the electrolyte (mainly ranging from 300 to 600 mL^{-1} and mostly finer than 5 μm) provide a very minor contribution to the total number (less than 1/20 of the cleanest sample's number concentration). The electrolyte provides an even weaker contribution to the total volume. This background is negligible and is not subtracted from our measurement results. Particle mass concentrations, C_m (μg kg^{-1}), were calculated from the volume sums, assuming a mean particle density of 2.6 g cm^{-3} (Sugimae, 1984). In this study, we define particles with diameters greater than 15 μm as 'coarse', while those greater than 30 μm (the limitation of the Coulter Counter measurement) are defined as 'giant'.

Though all the ice/firn cores were recovered from the glacier accumulation zone, post-depositional processes (e.g. melting, sublimation and snow redistribution on the glacier surface) might change the ice/firn core horizons to some degree. These processes are inevitable obstacles to the study of ice cores recovered from low-latitude mountains, especially those at relatively low altitudes. Sublimation at the surface of the glacier may smooth the oxygen isotopic variations and cause some annual dust-layer compaction (Thompson and others, 2006). Melting impacts on the water-soluble ions by elution. Though the effects of melting cannot be excluded, the annual cycles can be identified in the oxygen isotope ratio and/or impurities (ions and microparticles) profiles in most ice cores. In this paper, we study only the insoluble microparticles, which are the least mobile impurities in the ice core. Water-soluble particles or the soluble part of the microparticles dissolve in the meltwater and are lost during counting. The Muztagata, Everest and Dasuopu ice cores experienced less melting than the Dunde ice core, due to their much higher altitudes and larger annual accumulation rates. We believe the microparticle properties in the Tibetan Plateau ice cores are not substantially altered by possible post-depositional processes and can faithfully represent the insoluble atmospheric dust over those sites. These ice cores, though containing different time-spans, provide a long-term average of the present-day properties of the atmospheric dust over the sites.

RESULTS

The controls on oxygen isotopes across the Tibetan Plateau show regional differences. In the southern Tibetan Plateau

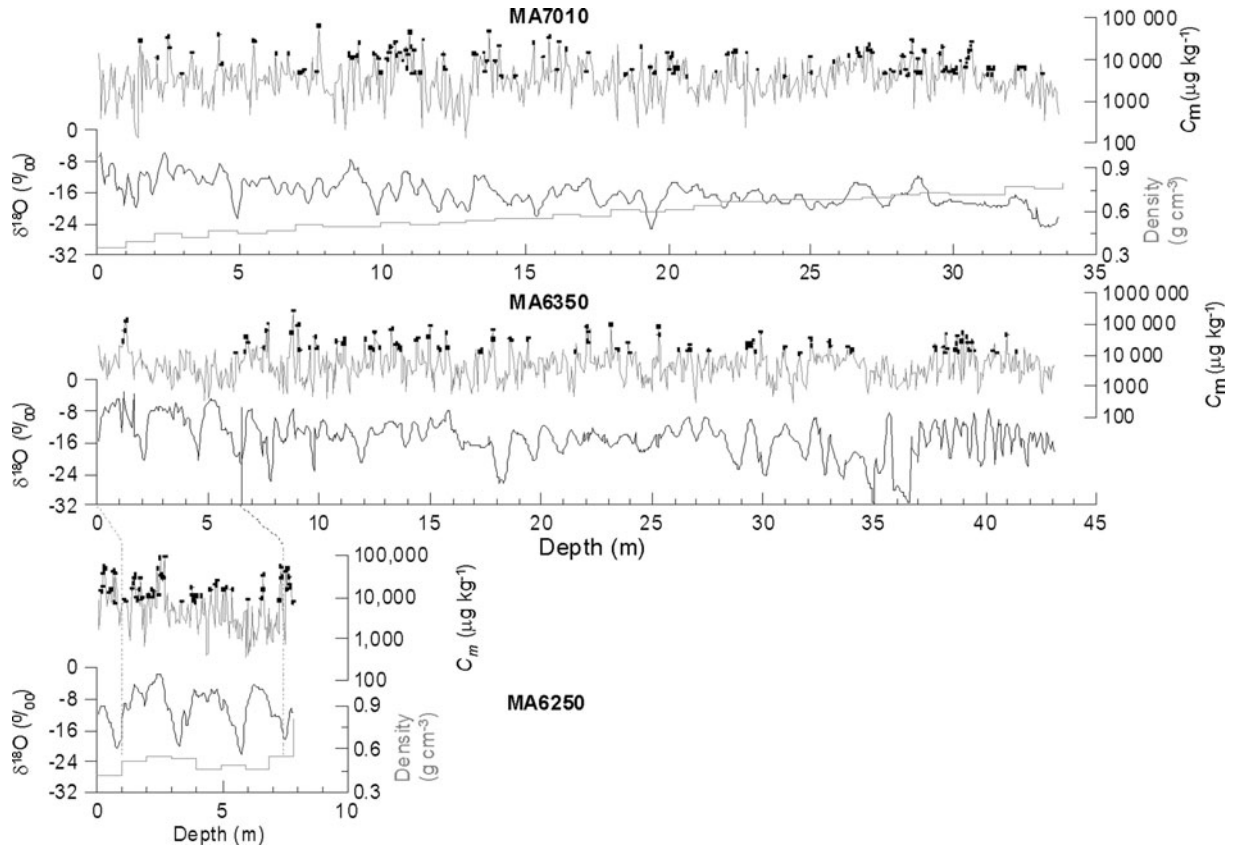

Fig. 2. Oxygen isotope ratios, density (grey curves) and microparticle mass concentrations (C_m) for the Muztagata ice cores. Black dots indicate the high C_m samples chosen for log-normal fitting.

(e.g. Dasuopu and Everest), the $\delta^{18}O$ ratio in precipitation is mainly influenced by the amount of precipitation, with high values during the winter (non-monsoon) season and low values during the summer (monsoon) season (e.g. Thompson and others, 2000). At Everest and Dasuopu, the non-monsoonal precipitation has $\delta^{18}O$ enrichment and high dust concentrations during the winter dry season, and $\delta^{18}O$ depletion and low dust concentrations during the wet monsoon season. The $\delta^{18}O$ ratio in precipitation in the northern and western Tibetan Plateau is primarily controlled by air temperature, with high $\delta^{18}O$ values found in summer precipitation and low $\delta^{18}O$ values found in winter precipitation (Thompson and others, 1988; Yao and others, 1996; Tian and others, 2006). At Muztagata, high dust concentrations occur mainly during summer, consistent with the frequency of dust storms in its source areas, such as the Pamirs, Afghanistan and Tajikistan (Wu and others, 2009).

The microparticles in ice cores from polar regions (Steffensen, 1997; Zielinski and Mershon, 1997; Zdanowicz and others, 1998; Delmonte and others, 2002; Ruth and others, 2003) show a strong log-normal volume distribution, which can be expressed as

$$\frac{\mathrm{d}V}{\mathrm{d}\ln D} = \frac{V_{\mathrm{Total}}}{\sqrt{2\pi}\ln\sigma}\exp\left[-\frac{1}{2}\left(\frac{\ln D - \ln D_{\mathrm{m}}}{\ln\sigma}\right)^2\right].$$

D is the particle diameter, D_{m} the mode, σ the standard deviation (SD) and V_{Total} the total volume. The log-normal fit can be described by three parameters: the mode, the SD and V. We discuss C_{m} (mass concentrations) rather than V. The volume (mass) fraction of the coarse particles (>15 μm) was calculated to check their contribution to the total mass. Furthermore, the coefficient of determination, R^2 for a log-normal fit, is also presented in order to check how well the measured size distribution correlates with the theoretical log-normal function. For each ice core, we chose samples from the highest C_{m} down to the lowest to compute the log-normal fit. Figures 2 and 3 illustrate the positions of the fitted high-concentration samples. Before the log-normal fitting process, the 300 size channels were combined to produce 50 channels. This channel width setting has an insignificant effect on the fitting result, because the mode and SD are essentially unchanged. In this study, the samples with R^2 for log-normal fit <0.6 were thought not to be of typical log-normal distribution and were discarded. This was an arbitrary standard. The measurement results show that some channels have no counts, i.e. particles in these channels contribute nothing to the total volume, whereas in a log-normal fit, the volume distribution is continuous. The vacant counts in some channels will yield discrepancies in the fitting results. The statistics of those fitting log-normal parameters for each ice core are listed in Table 1.

Coarse and giant particles clearly exist in these ice-core samples. Black, yellow and gray silt particles can be seen by the naked eye in melted samples. Scanning electronic microscope (SEM) photos (Fig. 4) clearly illustrate that many ultra-fine (<1 μm) and giant (>30 μm) particles also exist, though they were not measured due to the limitation of the Coulter Counter. The ultra-fine particles make a very small contribution to the total mass and have a very weak impact on volume distribution for the samples with high concentration. In contrast, a few coarse or giant particles of unusually large size have far greater influence on the total volume than do thousands of ultra-fine particles. For

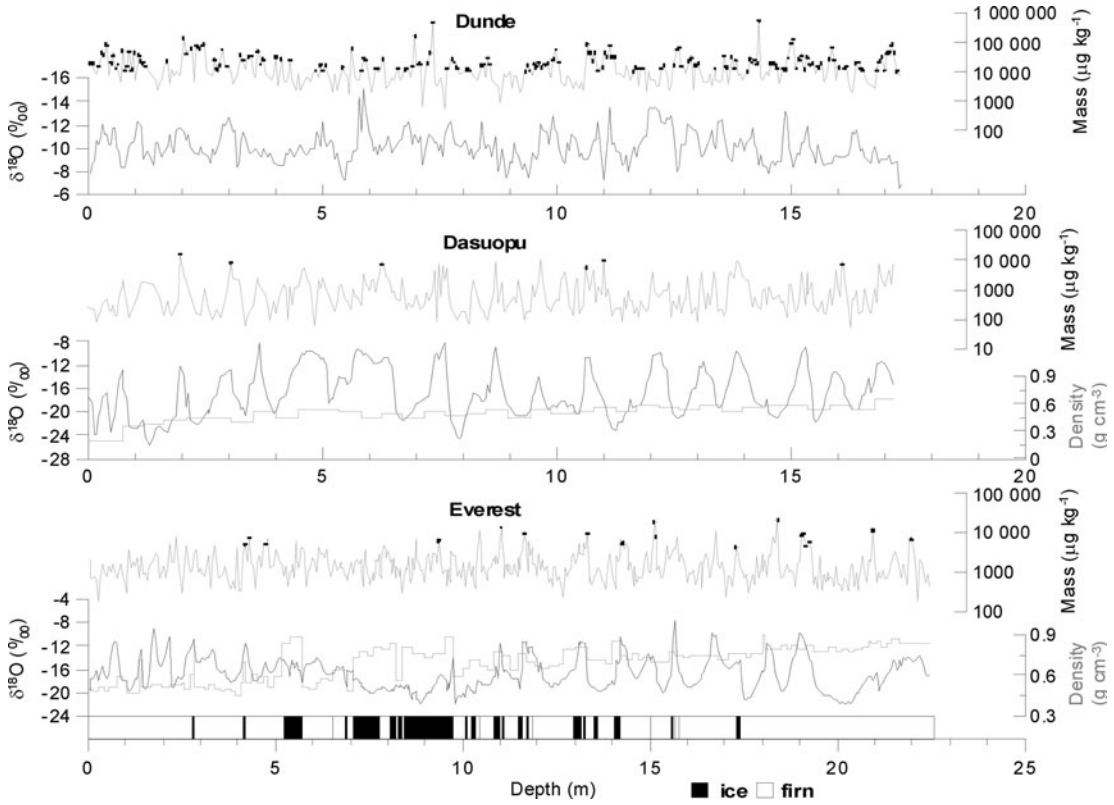

Fig. 3. Oxygen isotope ratios, density (grey curves) and microparticle C_m for the Dunde, Dasuopu and Everest ice cores. Black dots indicate the high-C_m samples chosen for log-normal fitting.The stratgraphy of the Everest ice core is also plotted.

example, in the Muztagata 6350 m a.s.l. ice core (hereinafter MA6350), a particle with a 16.15 μm diameter (1 out of a total number of 1928 particles) comprises 26% of the total volume of a sample, while a particle with a 15.63 μm diameter (1 out of a total number of 1310) accounts for over 30%. We chose two samples, one with high concentration (average $C_m = 3203\ \mu g\ kg^{-1}$) and another with low concentration (average $C_m = 1007\ \mu g\ kg^{-1}$) to be counted many times in order to assess the measurement error. We find that the count has the smallest error (6.4% for low C_m and 2.4% for high C_m), the surface area has a larger error (10.7% for low C_m and 5.6% for high C_m) and the volume has the greatest error (22.2% for low C_m and 9.5% for high C_m). There are two reasons for this: first, the coarse particles, which very possibly might pass through the aperture, contribute greatly to volume and surface area but not much to the total number; second, particles settle down during repeated counting, as shown by the decreasing trend in number, surface area and volume in the measurement. Generally, the measurement error for volume will decrease with increasing particle concentration.

DISCUSSION

Size distribution of microparticles in the ice cores

The ice-core samples span a range of three orders of magnitude in C_m (10^2–$10^5\ \mu g\ kg^{-1}$; Figs 2 and 3). In Figure 5, the low-concentration samples exhibit abnormal volume (mass) distributions and show no systematic characteristics, mostly exhibiting a low positive slope with particles existing sparsely in higher channels. A few of the clearer samples show that most of the volume consists of fine particles ranging between 1 and 3 μm. This phenomenon has also been reported for particles between 0.63 and 16 μm in other ice cores from the Tibetan Plateau (Davis, 2002). The irregularity in size distribution for microparticles from the

Table 1. Statistical results for the log-normal fitting parameters for particles in ice cores from the Tibetan Plateau

Site	*n*	Mode				SD				>15 μm mass			
		Range μm	Mean μm	SD μm	Median μm	Range	Mean	SD	Median	Range %	Mean %	SD %	Median %
MA6250	60	3.68–8.87	5.87	1.23	5.77	1.71–2.94	2.07	0.25	2.03	0–18.37	4.78	3.55	4.38
MA6350	101	3.23–10.49	5.74	1.34	5.68	1.55–2.63	2.06	0.20	2.05	0–21.73	4.68	4.04	3.86
MA7010	129	3.02–7.52	4.99	1.00	5.06	1.75–2.42	2.05	0.15	2.04	0–11.97	2.46	2.52	1.99
Dunde	161	3.35–15.98	6.67	1.77	6.42	1.50–2.68	1.94	0.20	1.93	0–41.55	6.46	5.67	4.99
Everest	18	3.79–9.88	6.99	1.62	6.67	1.56–2.34	1.87	0.20	1.86	0–18.75	6.41	4.72	6.23
Dasuopu	6	3.45–13.22	6.89	3.59	6.10	1.34–2.18	1.84	0.30	1.87	0–28.50	7.62	10.65	4.44

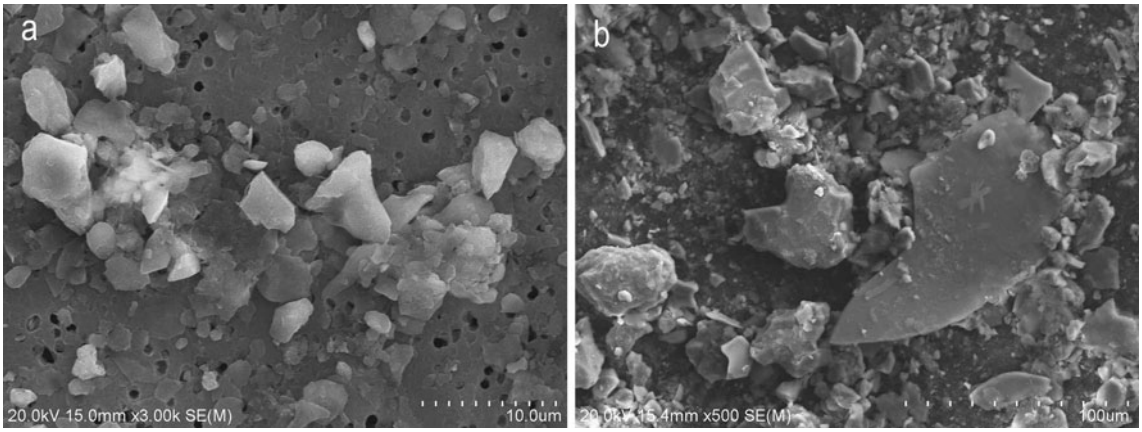

Fig. 4. SEM photos (from Dunde ice core (a) and MA6250 ice core (b)) for ultra-fine and giant particles collected on a Nuclepore membrane filter (Whatman Corporation, with pore size 0.8 μm diameter).

low-C_m samples is common in mountain ice cores, as indicated by reports from Hispar Glacier, Karakoram, and Ngozumpa Glacier, near Everest (Wake and others, 1994). This appears to be partly because a few, or even single, coarse particles comprise a large fraction of the total volume, although the coarse particles in the clear samples have a considerable uncertainty in volume measurement, as discussed above.

Almost all the dust particle size distributions of high C_m samples fit a log-normal size distribution well. The coarse particles (>15 μm) in these ice cores can constitute a large proportion of up to 40% of the total mass (volume). However, the average mass fraction of the >15 μm particles is generally minor, with about 2.5–7.6% of the total (Table 1). This indicates that the total mass is predominately dependent on the medium-size particles. In the Dunde ice core, the 3–15 μm particles contribute an average of $76 \pm 6\%$ (range 54–92%) to the total mass in the log-normal samples, while in the Muztagata 6250 m (MA6250), 6350 m (MA6350) and 7010 m (MA7010) ice cores, this proportion is $74 \pm 6\%$ (range 59–83%), $74 \pm 6\%$ (range 60–89%) and $71 \pm 7\%$ (range 53–84%), respectively. In the log-normal distribution, 68% of the total mass is in the 1σ size interval $[\exp(\ln D_m - \ln \sigma), \exp(\ln D_m + \ln \sigma)]$. The log-normal modes are mainly located in this 3–15 μm size range, and the 3–15 μm mass fraction (average ~71–76%) in these samples is similar to this value (68%). We conclude that the log-normal distribution is predominantly attributed to the mid-sized particles between 3 and 15 μm, which contribute most of the total volume.

The larger size of the mode of some samples arises from the effect of large particles that appear infrequently but make up a large fraction of the volume, instead of a continuous distribution of particles across all the measurement channels. Furthermore, though the log-normal distribution is widely used, it is neither exclusively suitable nor, in some cases, the best for describing atmospheric aerosol size distributions. The normal (Gaussian) distribution fits some high-concentration samples in those ice cores well (Wu, 2004).

The origin of coarse and giant particles in the ice cores (as shown in Fig. 4) is not clear. Dust-storm events on the Tibetan Plateau are frequent, though they are less frequent and less intense than those in the peripheral deserts. Satellite data show that the dust layers over the Tibetan Plateau appear most frequently around 4–7 km a.s.l. (Huang and others, 2007). The relative elevation between the bare

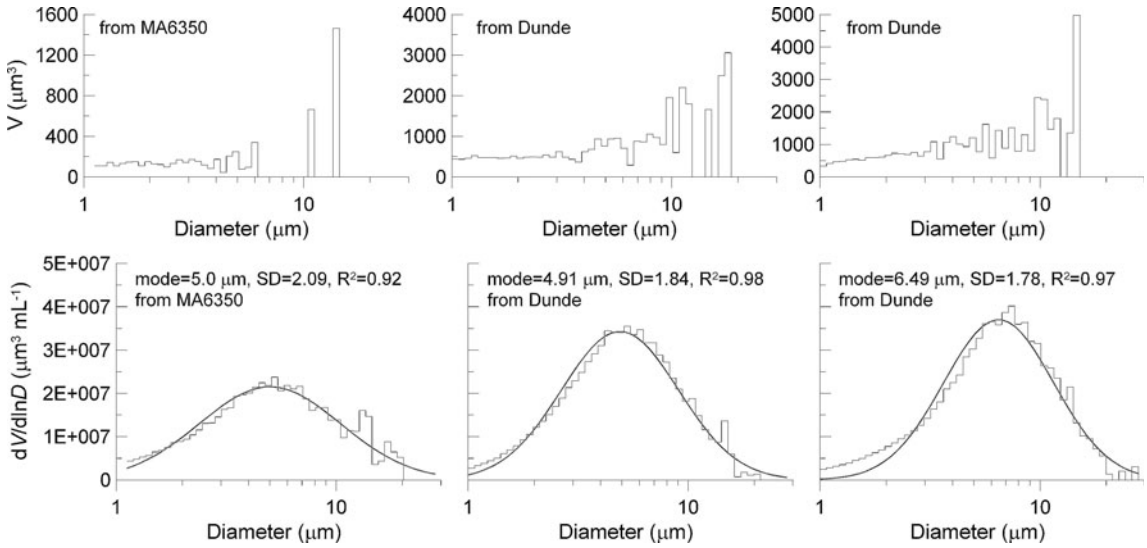

Fig. 5. Volume size distributions (in 50 channels on logarithmic scale) of microparticles in low- and high-C_m samples (black curves) and the log-normal fitting curves (grey curves) from the MA6350 and Dunde ice cores.

ground surface and the ice-core drilling site is ~3 km. Therefore, transport of local coarse material to the ice-core drilling site seems quite possible.

The coarse or giant particles can also come from a remote source hundreds or thousands of kilometers away. The giant particles (>62.5 μm), contrary to the traditional opinion that they will be preferentially removed by gravitational settling along the transport path, are found less often at greater distances (>1000 km) (Middleton and others, 2001), though the mechanism is not clear. Stokes gravitational settling overestimates the losses of large dust particles during atmospheric transport from North Africa over the tropical North Atlantic and Caribbean (Maring and others, 2003). On the Tibetan Plateau, the transport of coarse particles from local sources and areas remote from the glacier is therefore feasible. In an early dust-tracer transport model (GISS GCM) the calculated lifetime of silt was 179 hours for 2–3.6 μm and 28 hours for 12–20 μm particles (Tegen and Lacis, 1996). By contrast, in the late GISS GCM model, the silt fraction (8–16 μm) was supposed to have a gravitational deposition lifetime of 2.2 days (Miller and others, 2006). Dry deposition is less efficient in the current model, with a particle lifetime of 10.1 days (Miller and others, 2006), compared with the previous estimate of 8.9 days (Miller and others, 2004). The longer lifetime in the model allows dust particles to be transported over a longer range. The dust mass contributions from the lower, middle and upper troposphere in different size categories in the model show that most of the dust mass concentrates in the diameter range 1.2–6 μm (Miller and others, 2004). Our results show that for the high-concentration samples, which fit the log-normal law in volume size distribution, most of the mass is contained in the particle fraction of 3–15 μm diameter, which is much coarser than in the model. Our results also indicate that coarse particles might be common in the upper-level troposphere, at least over the Tibetan Plateau, and suggest that the lifetime of silt particles, especially the large ones, might still be underestimated, although we cannot discern the remote and local sources of these coarse/giant particles.

The complete size distribution for eolian dust may have three modes:

1. mode A, centered between 1 and 10 μm radius, which consists mainly of soil-derived aerosols under all conditions

2. mode B, centered between 10 and 100 μm radius, which may be the soil parent particles, and which appears only under heavy dust-loading conditions

3. mode C, centered between 0.02 and 0.5 μm radius, which might be the background aerosol and might be ambient (Patterson and Gillette, 1977).

We are aware that our measurements cover only particles in the range 1–30 μm, i.e. the mode A range, a small interval within the complete size range of atmospheric dust. Mode B particles, which are common in Chinese loess deposits, are less likely, but not impossible (as discussed above), to be found in the ice cores, owing to the difficulty of lifting and transporting parent soil particles at high elevation to the glacier. Mode C particles, the background aerosol (Ram and Gayley, 1994), are expected to exist in our samples, though they are too fine to be measured by Coulter Counter. Our results are strictly confined to the measured size range.

We need to pay attention to the possible solubility of some dust particles. If insoluble materials are internally mixed with a substantial amount of water-soluble materials, measurements of particle size by Coulter Counter will be biased to some degree, especially in Dasuopu and Everest where sea salts and anthropogenic substances might contribute a relatively higher proportion than at other sites. Aerosol collected in urban areas from a semi-arid region of western India indicates that the mineral dust component contributed to about 69% of the total suspended particles after neutralization by acidic pollutants (Rastogi and Sarin, 2006). However, due to the high altitude of ice-core sites and relatively weak anthropogenic effects, we believe that this issue is insignificant at the remote Everest/Dasuopu and other sites. Therefore, we consider that the measured size distribution is reliable.

The impact of altitude on size distribution

The MA6250, MA6350 and MA7010 ice-core samples from Muztagata provide a comparison for the impact of altitude on the mass concentration and size distribution of eolian dust deposited in alpine glaciers with similar air-mass trajectories (through the HYSPLIT model). The upper 6 m of the MA6350 ice core is found to correspond to the 0.8–7.5 m section of MA6250 core by matching the $\delta^{18}O$ profiles (Fig. 2, gray curves). These two sections show no significant difference in average C_m during the overlapping period (7466 μg kg^{-1} for the MA6350 section and 8893 μg kg^{-1} for the MA6250 section). However, many more samples that obey the log-normal size distribution were found in the MA6250 core than in the MA6350 core.

With increasing altitude, the log-normal distribution parameters also change, as the coarse particles settle out faster than finer particles. There is only a small difference in log-normal parameters between the MA6250 and MA6350 ice cores, with similar average mode (5.87 μm vs 5.74 μm), standard deviation (SD) (2.07 vs 2.06) and >15 μm mass percentage (4.78% vs 4.68%) (Table 1). We thus discuss the altitude impact focusing on the difference between the MA6250/MA6350 cores considered together and the MA7010 ice core (Table 1; Fig. 6):

1. The mode is smaller and less variable in the high-altitude ice core than in the lower ice cores. Particles from the MA7010 ice core have a mean mode of 4.99 μm (range 3.02–7.52 μm), while particles from MA6250 and MA6350 ice cores have mean modes of 5.87 μm (range 3.68–8.87 μm) and 5.74 μm (range 3.23–10.49 μm) respectively. The t test verifies that there is a significant difference between the MA6350 and MA7010 modes ($P = 2.8 \times 10^{-6} \ll 0.05$).

2. The three Muztagata ice cores show very similar SD (t test: $P = 0.43 \gg 0.05$) for the log-normal fit, indicating that elevation has no clear impact on this parameter.

3. The mass contribution of coarse particles in the MA7010 ice core is lower than in the MA6250/MA6350 cores, indicating that coarser particles make up a relatively smaller fraction of the total mass at higher altitude than at lower altitude.

4. Samples with lower C_m exhibit log-normal size distributions at greater altitude than those at lower elevations. In MA7010, dust concentrations as low as 4000 μg kg^{-1} can

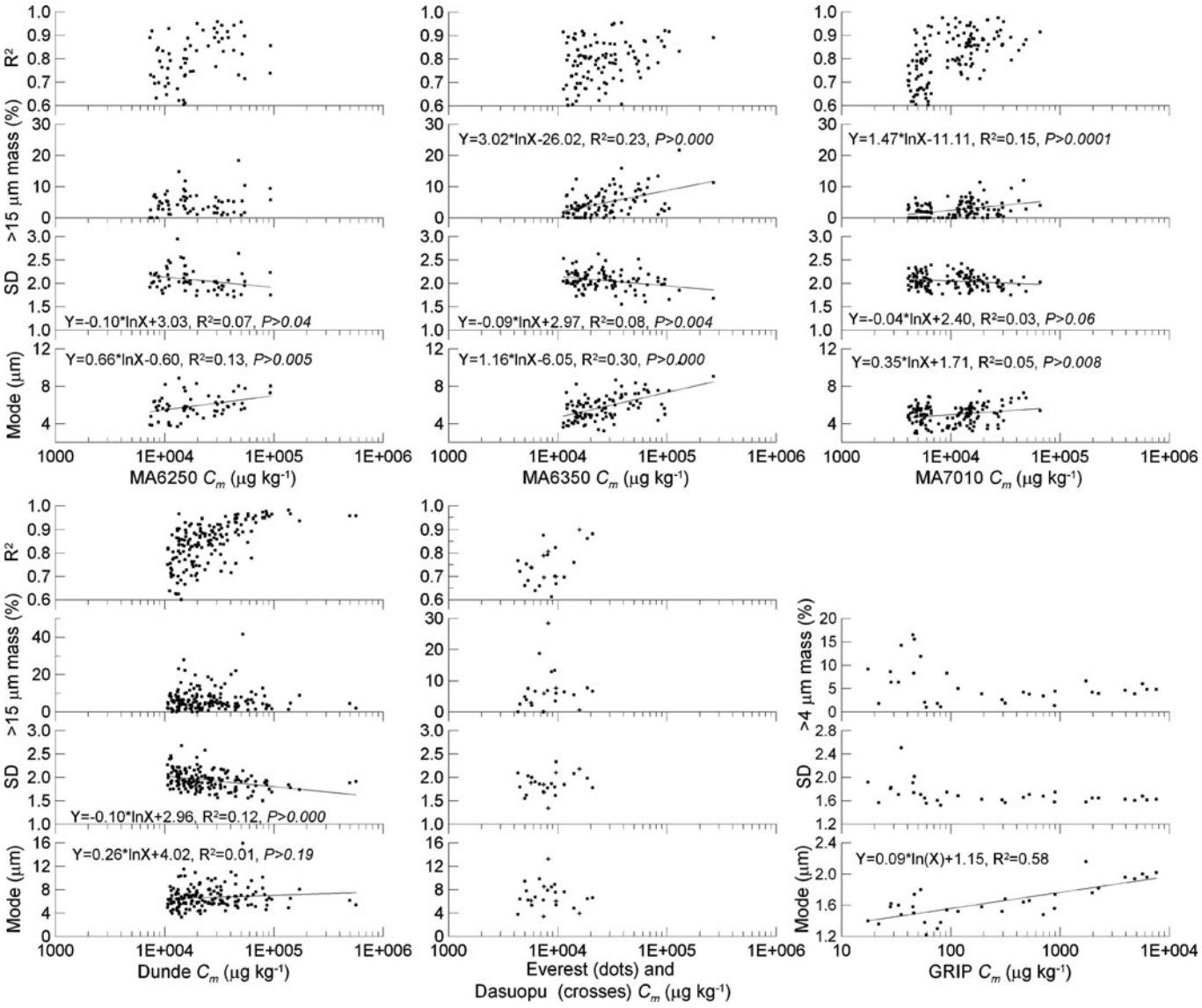

Fig. 6. Log-normal fitting parameters (the mode, SD, >15 um mass fraction and determination coefficient R^2) vs C_m (x axis; unit: μg kg^{-1}) for microparticles from ice cores on the Tibetan Plateau. The result from the GRIP ice core (Steffensen, 1997) is also shown for comparison. The line in each panel indicates the trend.

exhibit strong log-normal size distributions, while in MA6250 the C_m must be >7000 μg kg^{-1} to be well described as log-normal. This also indicates more extensive sorting at higher-altitude sites.

These log-normal parameter characteristics indicate that with increasing elevation of deposition, microparticles at higher altitude are more extensively sorted during transport and their size distribution more closely mimics a log-normal distribution. In addition, the size of the distribution mode trends smaller, with less variable SD and higher R^2 (Fig. 6). Our measurement is consistent with the modeled dust size distribution with height, which showed that modal size decreased quickly from 3.0 μm at 970 hPa to 1.6 μm at 470 hPa altitude (Tegen and Lacis, 1996).

Log-normal size distribution parameters

The parameters describing the log-normal fitting of dust size distributions provide additional insight into the characteristics of eolian dust. Particles in the Greenland ice cores (Zielinski and Mershon, 1997), as the end members of Asian dust, show a distinct log-normal distribution with a mode size commonly of ~2 μm. In the Greenland Icecore Project (GRIP) ice core (Fig. 6), microparticles show a log-normal distribution in the size interval 0.4–6 μm with nearly identical shapes, in spite of the large variability in C_m ranging from 10 to almost 10^4 μg kg^{-1} (Steffensen, 1997). Samples with very low C_m (only tens of μg kg^{-1}) have unimodal log-normal distributions similar to those with high dust concentration (thousands of μg kg^{-1}). This characteristic is also found in the NorthGRIP (Ruth and others, 2003) and Antarctic (Delmonte and others, 2002) ice cores, indicating that, after long-range transport, atmospheric dust is well sorted and can reach an equilibrium state with uniform and log-normal size distributions in some cases. In the GRIP ice core, as shown in Figures 6 and 7, the mode increases with increasing C_m, while the SD shows no correlation with C_m and remains relatively constant at about 1.6 μm. In addition, for those samples with C_m greater than 100 μg kg^{-1}, the SD and coarse (>4 μm) mass fraction seem to be constant. Consequently, a relatively constant SD and increasing mode size would result in a broader log-normal distribution with increasing C_m.

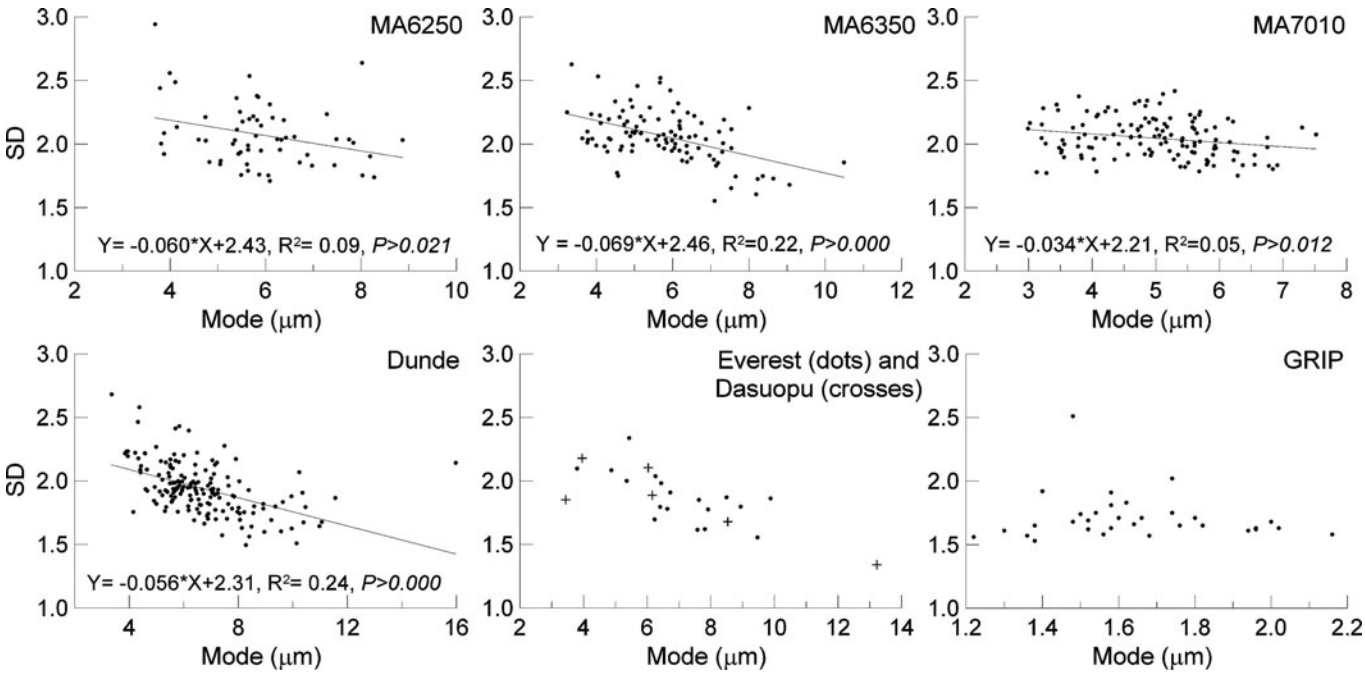

Fig. 7. The relation between the mode and SD in the ice-core samples from the Tibetan Plateau. The result from the GRIP ice core (Steffensen, 1997) is also shown for comparison. The line in (a–d) indicates the trend.

However, the observed size distribution of microparticles from the Tibetan Plateau ice cores does not demonstrate the same trend. The dust particle size distribution parameters in Figure 6 show that the microparticle size distributions become more log-normal when C_m increases in samples from all the sites, and especially those in the Dunde ice core. In contrast to the end members of the Asian dust in Greenland, the standard deviation of dust over the Tibetan Plateau decreases with increasing mass concentration. This suggests that the size distributions of microparticles in mountain ice cores differ from those in Greenland due to different effects of altitude and distance. R^2 becomes higher and the SD of the log-normal fitting generally decreases with increasing C_m. In all the Tibetan ice-core samples, the SD decreases with increasing mode size (Fig. 7), indicating that samples with larger mode sizes have volume distributions more concentrated in the log-normal part of the dust size distribution than those with smaller modes. This trend is much clearer in the Dunde ice core, a location surrounded by Asian dust-source areas. The correlation between the log-normal distribution parameters and mass concentration would help to simplify the characterization of dust used in general climate models.

Seasonal differentiation of dust particle volume size distribution

The mean number diameter and mean mass (volume) diameter of dust particles in ice cores on the Tibetan Plateau vary significantly on a seasonal basis (e.g. Wu and others, 2006). The seasonality of size distribution variability is also important in evaluating the radiative properties of atmospheric dust, especially for those sites where the prevailing circulations change seasonally. Differences in the log-normal fitting of samples from the spring–summer and autumn–winter seasons are clear in recent snows from the GRIP site (Steffensen, 1997). Though the Dasuopu ice core demonstrates the most obvious seasonal variation in $\delta^{18}O$ and dust concentration profile (Fig. 3), only a few samples are well modeled by a log-normal size distribution. Here we investigate the seasonal variability in dust size distribution parameters using the well-dated MA6250 ice-core record, which has clear seasonality in $\delta^{18}O$ values and finely resolved vertical sampling.

Samples well modeled by a log-normal distribution can occur during both the winter and summer seasons in the MA6250 ice core (Fig. 8). Although this record is subject to some uncertainties owing to limited data from only one site and a relatively short time-span, the results indicate that the seasonal differences in the log-normal fitting parameters appear to be minor and no systematic trend is obvious. Generally, in all the cores studied in this paper, no obvious systematic correlations between the log-normal parameters and oxygen isotope ratios were evident. Therefore log-normal fitting parameters appear more dependent on dust-storm events rather than season. Dust-storm events occur mainly during the dust season, but they can also occur, though less frequently, throughout the year. We suspect that weak dust-storm events loft only a small amount of dust particles into the atmosphere and do not produce the log-normal distribution. However, the detailed physical processes that lead to a strong dust storm creating a log-normal distribution still elude us.

Regional differences of log-normal characteristics

Wake and others (1994) pointed out that the observed size distribution of microparticles from ice cores in the Tibetan Plateau is dependent upon physiographic location with respect to dust source regions and atmospheric transport pathways. For example, the size distribution of the dust in the northern and western Tibetan Plateau, such as that from Muztagata and nearby Congce, appears to be log-normal, while the dust in the southern Himalaya shows a slightly positive slope (volume increases with increasing diameter) in volume-size distribution.

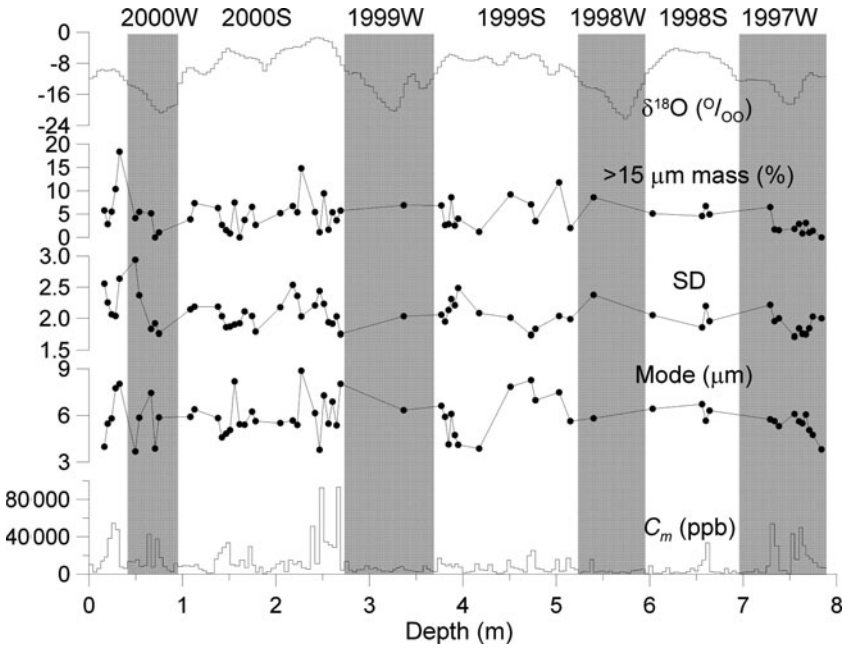

Fig. 8. The time series of oxygen isotope ratios ($\delta^{18}O$) and log-normal parameters from the MA6350 ice core. W and S indicate winter season (grey area) and summer season respectively.

Our results indicate the volume size distribution tends toward log-normal depending on dust mass concentration but is independent of physiographical location. The sites of the Everest and Dasuopu ice cores located in the southern part of the Tibetan Plateau have similar climate and landscape. We designated the combination of these two ice cores with different symbols (Figs 6 and 7) to represent the atmospheric dust over the central Himalaya. The three sites with different climate regimes on the Tibetan Plateau, namely Dunde, Muztagata and Dasuopu/Everest, provide a regional view of the dust particle size distribution. In the northern (Dunde) and western (Muztagata) Tibetan Plateau, adjacent to the Asian dust-source areas, dust particles have a clear monomodal size distribution, and no bi- or multimodal distributions were found in the range of measurement (1–30 μm). In the southern Tibetan Plateau, high-concentration samples from Everest and Dasuopu also have a monomodal log-normal distribution, while some samples have clear bi- or polymodal size distributions, though the C_m is low. Aerosols collected in Nepal indicate that desert dust can be transported regionally as well as long distances (possibly from the Sahara) to the Himalaya (Carrico and others, 2003). In the Himalaya, the mixture of dust particles from both local and remote sources may combine to produce a multimodal size distribution. Bimodal size distribution of Asian dust can be found in some ice cores (Wake and others, 1994) and loess sediments (Sun and others, 2002). The dust concentration and polymodal size distribution for microparticles in the Everest and Dasuopu ice cores will be discussed in further work.

SUMMARY AND CONCLUSION

This study of microparticles from several shallow ice cores on the Tibetan Plateau reveals the detailed characteristics of modern High Asia atmospheric dust in the upper-level troposphere and shows how the size distributions differ at those remote sites. Several summaries and conclusions can be drawn:

1. Our results reveal that whether the volume-size distribution fits the log-normal function largely depends on the dust concentration and the specific dust-storm event but is independent of physiographical location and season.

2. Only high-concentration samples obey the log-normal distribution in volume, with mode sizes ranging from 3 to 16 μm. The log-normal distribution was largely attributed to the mid-sized particles between 3 and 15 μm, which contribute a majority (>70%) of the total volume.

3. The standard deviation of dust over the Tibetan Plateau decreases with increasing mass concentration. The standard deviation for log-normal distribution at different sites and different altitudes centers at about 2 μm.

4. The volume-size distribution characteristics for mineral dust particles from ice cores reveal that the coarse particles are common in the upper-level troposphere over the Tibetan Plateau. This suggests that the lifetime of silt particles in the atmosphere, especially for the large particles, might still be underestimated in current models.

ACKNOWLEDGEMENTS

We thank the team members for ice-core drilling on the Tibetan Plateau. We also thank B. Delmonte, H. Maring, two anonymous reviewers and the Scientific Editor, D. Peel, for constructive and helpful comments and suggestions, and G. Hodgson and H. Maring for improving the text. This work is supported by the National Natural Science Foundation of China (grant Nos. 40871046 and 40571038) and the National Basic Research Program of China (grant No. 2005CB422004).

REFERENCES

Arimoto, R., B.J. Ray, N.F. Lewis, U. Tomza and R.A. Duce. 1997. Mass-particle size distributions of atmospheric dust and the dry deposition of dust to the remote ocean. *J. Geophys. Res.,* **102**(D13), 15,867–15,874.

Carrico, C.M., M.H. Bergin, A.B. Shrestha, J.E. Dibb, L. Gomes and J.M. Harris. 2003. The importance of carbon and mineral dust to seasonal aerosol properties in the Nepal Himalaya. *Atmos. Environ.,* **37**(20), 2811–2824.

Davis, M.E. 2002. Climatic interpretations of eolian dust records from low-latitude, high altitude ice cores. (PhD thesis, Ohio State University.)

Delmonte, B., J.R. Petit and V. Maggi. 2002. Glacial to Holocene implications of the new 27000-year dust record from the EPICA Dome C (East Antarctica) ice core. *Climate Dyn.,* **18**(8), 647–660.

Fang, X., Y. Han, J. Ma, L. Song, S. Yang and X. Zhang. 2004. Dust storms and loess accumulation on the Tibetan Plateau: a case study of dust event on 4 March 2003 in Lhasa. *Chinese Sci. Bull.,* **49**(9), 953–960.

Huang, J. *and 9 others*. 2007. Summer dust aerosols detected from CALIPSO over the Tibetan Plateau. *Geophys. Res. Lett.,* **34**(18), L18805. (10.1029/2007GL029938.)

Junge, C.E. 1977. Processes responsible for the trace content in precipitation. *IAHS Publ.* 118 (Symposium at Grenoble, 1975 – *Isotopes and Impurities in Snow and Ice*), 63–77.

Lau, K.M., M.K. Kim and K.M. Kim. 2006. Asian summer monsoon anomalies induced by aerosol direct forcing: the role of the Tibetan Plateau. *Climate Dyn.,* **26**(7–8), 855–864.

Maring, H., D.L. Savoie, M.A. Izaguirre, L. Custals and J.S. Reid. 2003. Mineral dust aerosol size distribution change during atmospheric transport. *J. Geophys. Res.,* **108**(D19), 8592. (10.1029/2002JD002536.)

Middleton, N.J., P.R. Betzer and P.A. Bull. 2001. Long-range transport of 'giant' aeolian quartz grains: linkage with discrete sedimentary sources and implications for protective particle transfer. *Mar. Geol.,* **177**(3–4), 411–417.

Miller, R.L., I. Tegen and J. Perlwitz. 2004. Surface radiative forcing by soil dust aerosols and the hydrologic cycle. *J. Geophys. Res.,* **109**(D4), D04203. (10.1029/2003JD004085.)

Miller, R.L. *and 10 others*. 2006. Mineral dust aerosols in the NASA Goddard Institute for Space Sciences ModelE atmospheric general circulation model. *J. Geophys. Res.,* **111**(D6), D06208. (10.1029/2005JD005796.)

Patterson, E.M. and D.A. Gillette. 1977. Commonalities in measured size distributions for aerosols having a soil-derived component. *J. Geophys. Res.,* **82**(15), 2074–2082.

Porter, S.C. and Z. An. 1995. Correlation between climate events in the North Atlantic and China during the last glaciation. *Nature,* **375**(6529), 305–308.

Ram, M. and R.I. Gayley. 1994. Insoluble particles in polar ice: identification and measurement of the insoluble background aerosol. *Geophys. Res. Lett.,* **21**(6), 437–440.

Rastogi, N. and M.M. Sarin. 2006. Chemistry of aerosols over a semi-arid region: evidence for acid neutralization by mineral dust. *Geophys. Res. Lett.,* **33**(23), L23815. (10.1029/2006GL027708.)

Rea, D.K. and S.A. Hovan. 1995. Grain size distribution and depositional processes of the mineral component of abyssal sediments: lessons from the North Pacific. *Paleoceanography,* **10**(2), 251–258.

Ruth, U., D. Wagenbach, J.P. Steffensen and M. Bigler. 2003. Continuous record of microparticle concentration and size distribution in the central Greenland NGRIP ice core during the last glacial period. *J. Geophys. Res.,* **108**(D3), 4098. (10.1029/2002JD002376.)

Shrestha, A.B. *and 6 others*. 2000. Seasonal variations in aerosol concentrations and compositions in the Nepal Himalaya. *Atmos. Environ.,* **34**(20), 3349–3363.

Steffensen, J.P. 1997. The size distribution of microparticles from selected segments of the GRIP ice core representing different climatic periods. *J. Geophys. Res.,* **102**(C12), 26,755–26,763.

Sugimae, A. 1984. Elemental constituents of atmospheric particulates and particle density. *Nature,* **307**(5947), 145–147.

Sun, D. *and 6 others*. 2002. Grain-size distribution function of polymodal sediments in hydraulic and aeolian environments, and numerical partitioning of the sedimentary components. *Sediment. Geol.,* **152**(3–4), 263–277.

Tegen, I. and A.A. Lacis. 1996. Modeling of particle size distribution and its influence on the radiative properties of mineral dust aerosol. *J. Geophys. Res.,* **101**(D14), 19,237–19,244.

Thompson, L.G., E. Mosley-Thompson, X. Wu and Z. Xie. 1988. Wisconsin/Würm glacial stage ice in the subtropical Dunde ice cap, China. *GeoJournal,* **17**(4), 517–523.

Thompson, L.G., T. Yao, E. Mosley-Thompson, M.E. Davis, K.A. Henderson and P. Lin. 2000. A high-resolution millennial record of the south Asian monsoon from Himalayan ice cores. *Science,* **289**(5486), 1916–1919.

Thompson, L.G. *and 7 others*. 2006. Holocene climate variability archived in the Purugangri ice cap on the central Tibetan plateau. *Ann. Glaciol.,* **43**, 61–69.

Tian, L. *and 8 others*. 2006. Recent rapid warming trend revealed from the isotopic record in Muztagata ice core, eastern Pamirs. *J. Geophys. Res.,* **111**(D13), D13103. (10.1029/2005JD006249.)

Wake, C.P., P.A. Mayewski, Z. Li, J. Han and D. Qin. 1994. Modern eolian dust deposition in central Asia. *Tellus,* **46B**(3), 220–233.

Wu, G.J. 2004. Study on microparticle in the Muztagata and Guliya ice cores. (Post-Doctoral Fellowship Research Report, Cold and Arid Regions Environmental and Engineering Research Institute, Chinese Academy of Sciences, Lanzhou.)

Wu, G. *and 6 others*. 2006. Grain size record of microparticles in the Muztagata ice core. *Sci. China D,* **49**(1), 10–17.

Wu, G., B. Xu, C. Zhang, S. Gao and T. Yao. 2009. Geochemistry of dust aerosol over the Eastern Pamirs. *Geochim. Cosmochim. Acta,* **73**(4), 977–989.

Yao, T., L.G. Thompson, E. Mosley-Thompson, Y. Zhihong, Z. Xingping and P.N. Lin. 1996. Climatological significance of $\delta^{18}O$ in north Tibetan ice cores. *J. Geophys. Res.,* **101**(D23), 29,531–29,537.

Zdanowicz, C.M., G.A. Zielinski and C.P. Wake. 1998. Characteristics of modern atmospheric dust deposition in snow on the Penny Ice Cap, Baffin Island, Arctic Canada. *Tellus,* **50B**(5), 506–520.

Zhang, X.Y., R. Arimoto and Z.S. An. 1999. Glacial and interglacial patterns for Asian dust transport. *Quat. Sci. Rev.,* **18**(6), 811–819.

Zielinski, G.A. and G.R. Mershon. 1997. Paleoenvironmental implications of the insoluble microparticle record in the GISP2 (Greenland) ice core during the rapidly changing climate of the Pleistocene–Holocene transition. *Geol. Soc. Am. Bull.,* **109**(5), 547–559.

MS received 7 November 2008 and accepted in revised form 28 September 2009